J. Fluid Mech. (1981), *vol.* 104, *pp.* 419–443
Printed in Great Britain

Fully developed MHD turbulence near critical magnetic Reynolds number

By J. LÉORAT,
Observatoire de Meudon, 92190 Meudon, France, and Université Paris VII
A. POUQUET AND U. FRISCH
Centre National de la Recherche Scientifique Observatoire de Nice, Nice, France

(Received 31 January 1980)

Liquid-sodium-cooled breeder reactors may soon be operating at magnetic Reynolds numbers R^M where magnetic fields can be self-excited by a dynamo mechanism (as first suggested by Bevir 1973). Such flows have kinetic Reynolds numbers R^V of the order of 10^7 and are therefore highly turbulent.

This leads us to investigate the behaviour of MHD turbulence with high R^V and low magnetic Prandtl numbers. We use the eddy-damped quasi-normal Markovian closure applied to the MHD equations. For simplicity we restrict ourselves to homogeneous and isotropic turbulence, but we do include helicity.

We obtain a critical magnetic Reynolds number R_c^M of the order of a few tens (non-helical case) above which magnetic energy is present. R_c^M is practically independent of R^V (in the range 40 to 10^6). R_c^M can be considerably decreased by the presence of helicity: when the overall size of the flow L is much larger than the integral scale l_0, R_c^M can drop below unity as suggested by an α-effect argument. When $L \approx l_0$ the drop can still be substantial (factor of 6) when helicity is a maximum. We examine how the turbulence is modified when R^M crosses R_c^M: presence of magnetic energy, decreased kinetic energy, steepening of kinetic-energy spectrum, etc.

We make no attempt to obtain quantitative estimates for a breeder reactor, but discuss some of the possible consequences of exceeding R_c^M, such as decreased turbulent heat transport. More precise information may be obtained from numerical simulations and experiments (including some in the subcritical regime).

1. Introduction

A common explanation of the magnetic fields observed on the Earth, the Sun and many other cosmic objects involving conducting fluid motion is the dynamo effect; when the magnetic Reynolds number R^M is sufficiently large, the stretching of magnetic field lines by velocity gradients may overcome the Joule dissipation. An arbitrary weak 'seed' field will then grow to a finite value and remain so as long as the flow is driven by some mechanism (Busse 1978; Moffatt 1978 and references therein).

In an astrophysical or geophysical context, magnetic Reynolds numbers are generally much greater than unity. The situation is very different when MHD experiments are performed in the laboratory (for example, with liquid metals such as mercury or sodium). There are no particular difficulties in achieving substantial kinetic Reynolds

0022-1120/81/4658-3400 $02.00

numbers, but the magnetic Reynolds numbers will generally be well below unity. This may be seen as a consequence of the smallness of the magnetic Prandtl number ν/λ (ν = kinematic viscosity, λ = magnetic diffusivity) of liquid metals, which is 10^{-7} for mercury at room temperature and 10^{-5} for liquid sodium at 100 °C. At small magnetic Reynolds numbers, MHD effects can be present only if an external magnetic field is prescribed, such as in the MHD turbulence experiment reported by Alemany *et al.* (1979).

As was pointed out first by Bevir (1973), a man-made dynamo involving only fluid motion could be the involuntary by-product of building large-scale breeder reactors (see also Pierson 1975; Gailitis, Freiberg & Lielausis 1977; Léorat, Pouquet & Frisch 1979); for example, the liquid-sodium-cooled breeder reactor Superphenix under construction at Malville (France) will achieve kinetic Reynolds numbers $R_L^V \simeq 10^7$ and in places, a magnetic Reynolds number R_L^M, of about 50. The present work was strongly motivated by this observation (which was brought to our attention by R. Moreau); however, we make no attempt to predict for Superphenix the precise value of the *critical* magnetic Reynolds number R_{Lc}^M, defined as the value of R_L^M above which a self-excited dynamo becomes possible (we shall come back in the conclusion, § 4, to what is involved in trying to make such a prediction). Our aim is to gain a better understanding of the physics of conducting flows at very low magnetic Prandtl numbers with high kinetic Reynolds numbers and magnetic Reynolds numbers near the critical value. Exactly what sort of questions we may hope to answer will be stated only after we have formulated the turbulent dynamo problem more precisely and discussed some of the existing results. This will be done in the remainder of this introduction.

The flow of an incompressible conducting fluid is governed by the MHD equations:

$$(\partial/\partial t - \nu\nabla^2)\,\mathbf{v} = -(\mathbf{v}\,.\,\nabla)\,\mathbf{v} - \nabla p + (\mathbf{b}\,.\,\nabla)\,\mathbf{b} + \mathbf{f}, \tag{1.1}$$

$$(\partial/\partial t - \lambda\nabla^2)\,\mathbf{b} = -(\mathbf{v}\,.\,\nabla)\,\mathbf{b} + (\mathbf{b}\,.\,\nabla)\,\mathbf{v}, \tag{1.2}$$

$$\nabla\,.\,\mathbf{v} = 0, \quad \nabla\,.\,\mathbf{b} = 0, \tag{1.3}$$

plus boundary and initial conditions; $\mathbf{v}$ is the velocity, $\mathbf{b}$ the magnetic field (rescaled to make it an Alfvén velocity) and $\mathbf{f}$ an external force.

From the linearity in $\mathbf{b}$ of the induction equation (1.2) it is clear that, when there is no externally prescribed magnetic field present at the boundaries, the MHD equations admit non-magnetic solutions where $\mathbf{b} \equiv 0$ and $\mathbf{v}$ is a solution of the Navier–Stokes equation for non-conducting fluids. Let us assume that the force and the boundary conditions are such that the Navier–Stokes equation has a steady-state non-vanishing hydrodynamic solution. This can be a deterministic steady state with a time-independent velocity field (typically at low kinetic Reynolds numbers) or a statistical steady state (high kinetic Reynolds numbers) where the velocity is a random function stationary in time. In this paper, we shall assume that randomness is established by driving the flow with prescribed stochastic forces which are stationary and homogeneous. It is conceivable that stochasticity in many MHD flows is of intrinsic nature. This is the case for a number of simple model systems where a 'strange attractor' has been found (Lorenz 1963; Ruelle & Takens 1971; Martin 1976).

The (turbulent) dynamo problem concerns the stability of the $\mathbf{b} = 0$ solution: if a very weak 'seed' magnetic field is introduced at some time $t = t_0$, will it eventually

($t \to \infty$) decay to zero or will a new steady state be obtained with non-vanishing magnetic field and (generally) modified velocity field? An equivalent question is to have at all times a prescribed magnetic field $\epsilon \mathbf{B}_0$ ($\epsilon \ll 1$) and to ask whether the steady state has a magnetic field $O(\epsilon)$ or $O(1)$. As is well known, if one is only interested in the stability of the solution and not in the modified magnetic steady state, the dynamo problem can be analysed in the so-called kinematical framework, where the velocity field is prescribed and only the induction equation (1.2) is studied. The existence of the dynamo effect has been demonstrated analytically with suitably chosen velocity fields (see, for example, Backus 1958) and numerically by integration of the induction equation (see, for example, Gubbins 1973). Numerically determined critical magnetic Reynolds numbers R_{Lc}^M are often found in the range 10–100 (Roberts 1972; Gubbins 1973; Pekeris, Accad & Shkoller 1973). Although this is precisely the range where Superphenix should be operating, the relevance is not immediately clear because all existing calculations assume velocity fields with only a few scales of motion, which are not at all typical of flows at high kinetic Reynolds number.

A turbulent flow may have three very distinct characteristic scales: (i) the overall scale of the flow L; (ii) the integral scale l_0, characteristic of energy-carrying eddies, which we shall use henceforth to define kinetic and magnetic Reynolds numbers

$$R^V = l_0 v_0/\nu, \quad R^M = l_0 v_0/\lambda, \tag{1.4}$$

where v_0 is the r.m.s. velocity; (iii) the dissipation scale l_d below which viscous effects become important. According to the Kolmogorov (1941) theory

$$l_0/l_d \approx (R^V)^{\frac{3}{4}}. \tag{1.5}$$

A possible small deviation from the $\frac{3}{4}$ exponent in (1.5) due to intermittency (Kolmogorov 1962; Frisch, Sulem & Nelkin 1978) seems of little relevance in the present context.

Given the presence of three characteristic scales in the system, it is not immediately clear how we can construct a dimensionless number governing the dynamo effect (when such an effect exists). In a flow where $L \approx l_0 \approx l_d$, for dimensional reasons, the critical magnetic Reynolds number R_c^M, if it exists, must be a pure number. This is no longer so in a turbulent flow with two or three different characteristic scales: R_c^M may then functionally depend on L/l_0 and l_0/l_d. Some understanding of what the relevant parameters are can be obtained by using simple phenomenological arguments, most of which are rather standard (Kraichnan & Nagarajan 1967; Moffatt 1978 and references therein). It is useful to think of the induction equation (1.2) as describing a competition between (i) spatial transport of magnetic fields ($\mathbf{v} \cdot \nabla \mathbf{b}$ term), (ii) stretching of field lines by velocity gradients ($\mathbf{b} \cdot \nabla \mathbf{v}$ term), (iii) Joule dissipation ($\lambda \nabla^2 \mathbf{b}$ term). The rate of stretching is at most $\sup |\nabla \mathbf{v}|$ (which we use here as a shorthand notation for the largest eigenvalue of the rate-of-strain tensor). The rate of dissipation, because it varies like the inverse square of the scale of the currents is, at least, λL^{-2}. This suggests as a *necessary* condition for a dynamo effect

$$\sup |\nabla \mathbf{v}| \, L^2/\lambda \gtrsim 1. \tag{1.6}$$

That (1.6) is indeed a necessary condition has been shown from a rigorous energy-type proof by Backus (1958). For high kinetic Reynolds numbers, we can estimate $\sup |\nabla \mathbf{v}|$ using the Kolmogorov (1941) theory; this gives us the inverse of the eddy-turnover

time evaluated at the dissipation scale l_d. The Backus necessary condition for dynamo effect becomes then

$$R^M(L/l_0)^2\,(l_0/l_d)^{\frac{2}{3}} \approx R^M(R^V)^{\frac{1}{2}}\,(L/l_0)^2 \gtrsim 1, \tag{1.7}$$

where R^M and R^V are based on the integral scale (definitions 1.4). A criticality criterion involving a competition between stretching at scales $\approx L$ and dissipation at scales $\approx l_d$ should leave considerable room for improvement of (1.7). A much more stringent necessary condition for the dynamo effect is indeed provided by the Childress (1969) criterion, also based on a rigorous energy-type estimate:

$$\sup|\mathbf{v}|\,L/\lambda \approx R^M L/l_0 \gtrsim 1. \tag{1.8}$$

To get a better evaluation of R_c^M, it is tempting to compare at each scale l in the inertial range, the local stretching rate (the inverse of the local eddy-turnover time) with the local dissipation rate λl^{-2}. Using again Kolmogorov (1941) estimates, we find that growth should take place at scales l such that

$$(v_0/l_0)\,(l/l_0)^{-\frac{2}{3}}\,(\lambda l^{-2})^{-1} \gtrsim 1. \tag{1.9}$$

This is compatible with l being in the inertial range as soon as

$$R^M \gtrsim 1. \tag{1.10}$$

The trouble with the argument is that it completely ignores the effect of the advection term $(\mathbf{v}\,.\,\nabla)\,\mathbf{b}$ in the equation (1.2). Advection by a random velocity field does not directly change field strength but it is able to transfer magnetic energy from one scale to another. As we shall now see, this can be a source sometimes of enhanced damping and sometimes of enhanced growth of the field.

Enhanced damping is due to an eddy-diffusivity mechanism: the advection by a random velocity field results in transfer of magnetic energy to small scales where it can be rapidly Joule dissipated. The magnetic eddy diffusivity appropriate for scales $\approx l_0$ can be estimated by a standard random-walk argument,

$$\lambda_{\mathbf{eddy}} \approx l_0 v_0. \tag{1.11}$$

The corresponding eddy-dissipation rate for scales $\approx l_0$ is v_0/l_0, the same as the rate of stretching. As noticed by Kraichnan & Nagarajan (1967), with two competing mechanisms of the same characteristic time, the outcome is unclear, however large the magnetic Reynolds number. Actually, the outcome seems to depend on the dimension of space. In two dimensions, there is an antidynamo theorem implying that, for any finite magnetic Reynolds number, the steady-state magnetic energy is zero (Zel'dovich 1956). Note however that initial growth of a seed field and existence of a very long non-zero magnetic-energy plateau are not ruled out (Pouquet 1978).

Enhanced growth of the magnetic field is known to take place in three-dimensional helical flows (Steenbeck, Krause & Rädler 1966; see Moffatt 1978 for review). More precisely, assume that the following two conditions are met: (i) the flow is not statistically mirror-symmetric, i.e. it has non-vanishing kinetic helicity

$$H^V = \tfrac{1}{2}\langle \mathbf{v}\,.\,\mathrm{curl}\,\mathbf{v}\rangle \neq 0; \tag{1.12}$$

(ii) there is scale separation, $L \gg l_0$. It may then be shown that, at scales l such that, $L > l \gg l_0$, the magnetic field satisfies, in the kinematical case, an equation of the form

$$\partial\mathbf{b}/\partial t = (\lambda + \lambda_{\mathbf{eddy}})\,\nabla^2\mathbf{b} + \alpha\nabla\times\mathbf{b}; \tag{1.13}$$

$\lambda_{\text{eddy}} \approx l_0 v_0$ is the turbulent magnetic diffusivity. The 'torsality' α is a pseudo-scalar, of the order of $H^V l_0/v_0$ at high R^M's and of the order of $H^V l_0^2/\lambda$ at low R^M's. The $\alpha \nabla \times \mathbf{b}$ term, which comes from the interplay of the stretching and the advection terms in the induction equation, induces growth of magnetic fields at scales $\approx l$ with a rate $\approx \alpha/l$. Since the diffusive damping rate is proportional to l^{-2}, growth will take over if sufficiently large scales are available. Specifically, growth requires

$$\alpha L/(\lambda + \lambda_{\text{eddy}}) \gtrsim 1. \tag{1.14}$$

Assuming maximal helicity ($|H^V| \approx v_0^2/l_0$) and using the low R^M expression for α, we find a critical magnetic Reynolds number

$$R_c^M \approx (l_0/L)^{\frac{1}{2}} \tag{1.15}$$

which is much smaller than unity.

Realistic flows generated in bounded vessels often have the integral scale l_0 of the same order of magnitude as the largest scale L in the flow. The above analysis is then no more relevant and we cannot infer the effect of the helicity on the critical magnetic Reynolds number. There are many other questions for which simple phenomenological arguments do not provide an answer. Here is a list of such questions motivated by the breeder reactor problem: is there a critical magnetic Reynolds number R_c^M in a non-helical flow at high kinetic Reynolds number? How does it depend on the kinetic Reynolds number? How is it affected by helicity? Then, assuming that R_c^M exists, there is a second group of questions: How is the turbulence modified for $R^M > R_c^M$? How much magnetic energy is there? Are kinetic and magnetic energy of the same order, as suggested in a somewhat different context by Batchelor (1950), Biermann & Schlüter (1951), Kraichnan & Nagarajan (1967), Pouquet, Frisch & Léorat (1976)? If the turbulent flow has no preferred direction (isotropy), does this symmetry carry over to the magnetic field or will there be a mean magnetic field, as in a ferromagnet below the Curie temperature? Is the kinetic energy modified from its sub-R_c^M value? Does the kinetic-energy spectrum still satisfy the Kolmogorov $k^{-\frac{5}{3}}$ law? Are the turbulent transport coefficients (of heat, momentum, etc.) modified? Note that the questions of the second group are beyond the scope of the kinematical approach and require the full nonlinear MHD equations.

We now examine the tools available for such investigations. Work in MHD turbulence started in the late forties (see, for example, the review of Von Neumann 1949). In spite of the great expectations generated by the Kolmogorov (1941) theory, no major breakthrough has occurred in the theory of hydrodynamic turbulence, much less so in MHD turbulence. For ordinary turbulence, we have at least a reasonable qualitative understanding based on phenomenological ideas (mixing length, eddy viscosity, turnover time, etc.). This allows us for example to calculate inhomogeneous flows using one-point closures (Launder, Reece & Rodi 1975). Success here can be explained schematically by the fact that in ordinary turbulence, where there is a simple dimensionless parameter (R^V), many quantities are uniquely determined by dimensional constraints (within pure numerical factors). In MHD turbulence much more insight is needed to overcome the indeterminacies arising from the presence of two fields and two dimensionless numbers, particularly so when the magnetic Prandtl number ν/λ is very small. Probably the safest way to gain insight, in principle, is to

make experiments or numerical simulations (we shall come back to this in the concluding section). A not so direct but much more tractable approach is based on two-point closures of the kind used in MHD by Kraichnan (1958), Orszag & Kruskal (1968), Kraichnan & Nagarajan (1967), Pouquet *et al.* (1976). (For general reviews of modern closures, see Leslie 1973; Orszag 1977; Rose & Sulem 1978.)

Let us briefly recall the ideas underlying the eddy-damped quasi-normal Markovian (EDQNM) closure, which we shall use in this paper (see Rose & Sulem 1978 for details in the hydrodynamic case and Pouquet *et al.* 1976, for the MHD case). An infinite hierarchy of $2, 3, 4, \ldots, n$ point correlation functions (cumulants) can be obtained from the MHD equations. This hierarchy is then truncated at the level of triple correlations (third-order cumulants) assuming that the terms involving fourth-order cumulants are representable as a modification (renormalization) of the viscous and diffusive damping rates of triple correlations. In other words, the old idea of eddy viscosity and diffusivity, used for example in the Prandtl mixing-length theory, is implemented at a higher level. Choices of the eddy-damping rates can be made which ensure that (i) the $k^{-\frac{5}{3}}$ Kolmogorov spectrum is obtained when $R^V \to \infty$ in the absence of magnetic field; (ii) in the MHD case, when $R^V \to \infty$ and $R^M \to \infty$, one obtains Kraichnan's (1965) $k^{-\frac{3}{2}}$ spectrum which takes into account the effect of Alfvén waves on the inertial range.

For homogeneous isotropic helical MHD turbulence, the EDQNM closure leads to a system of integrodifferential equations for kinetic and magnetic energy and helicity spectra (see Pouquet *et al.* 1976, and appendix of this paper). Numerical integration of such equations is feasible even at high Reynolds numbers. In the range where breeder reactors are likely to operate ($R^V \approx 10^7$, $R^M \approx$ 10–100), a typical run to obtain steady-state solutions takes less than a minute on IBM 370-168. Results of such calculations are reported in § 3.

Naturally, in having recourse to closure theory, we have to pay a price. Some questions we would like to ask become meaningless for homogeneous isotropic turbulence, such as: is there a symmetry-breaking mechanism leading to a preferred direction of the magnetic field? For quantitative questions (e.g. how much is the critical magnetic Reynolds number of this flow?), we can expect at best orders of magnitude. However we are still in a position to investigate semi-quantitative questions (what is the influence of R^V on R_c^M? What is the influence of helicity when there is no scale separation between overall size and integral scale? How is the turbulence affected above R_c^M? etc.). In § 4 we shall discuss some of the possible implications of the closure-based results but also address questions which are beyond the scope of closure, suggesting new lines of investigations.

2. Closure for homogeneous isotropic MHD turbulence

The EDQNM closure

We use a modified version of the eddy-damped quasi-normal Markovian (EDQNM) approximation of Orszag (1970). The MHD version of this method has been introduced in a previous paper (Pouquet *et al.* 1976, henceforth called I), and has been reviewed elsewhere (Pouquet 1980). Notice that, although the EDQNM equations involve somewhat arbitrary phenomenological elements (e.g. the eddy-relaxation rates), identical results (up to second order in powers of the nonlinear terms) are obtained in

perturbation theory starting from the primitive MHD equations (1.1)–(1.3). Several essential structural properties of these last equations are shared by the closure equations: conservation of total energy and magnetic helicity by the nonlinear interactions, existence of kinetic and magnetic helicity effects acting upon large-scale magnetic excitation (see I), absence of dynamo effect in the two-dimensional case (Pouquet 1978).

The EDQNM closure leads to a set of four coupled integrodifferential nonlinear equations for the kinetic and magnetic energy and helicity spectra. The full equations are given in the appendix in a slightly different form from that in I. Although some analytical results can be obtained from these equations (see I), study of magnetic criticality relies upon numerical techniques of integration which we shall now describe briefly.

Numerical procedure

Numerical calculations performed on the closure equations can be done at high Reynolds number, of the order of 10^6 or greater, as opposed to a few tens presently reached for three-dimensional direct integration of the primitive MHD equations. This is due to the description of homogeneous isotropic turbulence in terms of wavenumbers and to the smoothness of the spectra, allowing an exponential discretization in wavenumbers. To follow the evolution of an initial magnetic field towards a steady state, the spectral equations can be integrated in time. In the vicinity of the critical magnetic Reynolds number, henceforth called critical region ($R^M \simeq R_c^M$), characteristic time scales become very large and the study of stationary solutions is best obtained with an iterative method first introduced by Leith (1971) in the context of non-magnetic two-dimensional turbulence. Let us first outline the iterative procedure for non-helical non-magnetic turbulence. The EDQNM equations read

$$(\partial/\partial t + 2\nu k^2 - \mathscr{A}_k^V)\, E_k^V = \mathscr{B}_k^V + F_k^V, \tag{2.1}$$

where $\mathscr{A}_k^V$ and $\mathscr{B}_k^V$, which stem from the nonlinear terms, are expressible as integrals depending on the kinetic-energy spectra (see appendix for detailed expressions). $-\mathscr{A}_k^V$ is called the 'absorption' term (it reduces to a positive eddy-viscosity term when the mode k interacts with wavenumbers $p \gg k$); $\mathscr{B}_k^V$ is shown to be always positive and is called the 'emission' term; it represents an input of energy into the mode k by nonlinear interactions among all other modes. In the iterative scheme for stationary solutions the zeroth-order solution $F_k^V/(2\nu k^2)$ neglects nonlinearities; then the nth-order solution is used to calculate the $\mathscr{B}_k^V$'s and $\mathscr{A}_k^V$'s which respectively modify the force and the viscosity. At the $(n+1)$th order of iteration, the stationary kinetic-energy spectrum $E_k^V(n+1)$ is thus given by

$$E_k^V(n+1) = (\mathscr{B}_k^V(n) + F_k^V)/(2\nu k^2 - \mathscr{A}_k^V(n)). \tag{2.2}$$

The MHD version is a matrix extension of this procedure (see appendix). Use of the iterative method is straightforward in the non-helical case. In the presence of helicity, however, two problems arise: possible occurrence of negative energy spectral densities due to ill-suited starting spectra, and accumulation of magnetic excitation at the lowest wavenumber. The former problem is solved by introducing small corrective terms in the first few iterations, convergence thus being obtained in all cases. The latter problem arises because the inverse transfer by helicity effects leads to very high excitation near the minimum wavenumbers $k_{\min}$ (see I). This in turn affects adjacent wavenumbers.

		Spectral energy densities				Total
		$k = 0{\cdot}25$	$k = 1$	$k = 8$	$k = 64$	energy
3000 time steps	E^V	0·330	1·41	0·0241	$0{\cdot}66 \times 10^{-5}$	2·356
	E^M	$0{\cdot}619 \times 10^{-2}$	0·0737	0·0110	$0{\cdot}89 \times 10^{-7}$	0·479
180 iterations	E^V	0·333	1·40	0·024	$0{\cdot}44 \times 10^{-5}$	2·345
	E^M	$0{\cdot}608 \times 10^{-2}$	0·0742	0·0103	$0{\cdot}56 \times 10^{-7}$	0·473

TABLE 1. Comparison of temporal integration and iterative method in the critical region (non-helical turbulence; $k_{\min}/k_0 = 0{\cdot}25$, $k_{\max}/k_0 = 861$; $R^V = 2150$, $R^M = 43$). The iterative procedure is ten times faster than the time integration method in this case.

The lower truncation in wavenumber space is a numerical constraint contradictory to the hypothesis of unbounded turbulence. To handle this unphysical accumulation, a suitable boundary condition is introduced: the missing large scales ($0 < k < k_{\min}$) are parametrized by a magnetic helicity dissipation term on wavenumber $k_{\min}$, which compensates exactly the emission term $\tilde{\mathscr{D}}^M_{k_{\min}}$ (appendix, equation (A 8)). Comparison between integration in time and the iterative method is given in table 1 for magnetic non-helical turbulence. Iteration is stopped when the relative variations of the magnetic and kinetic energies are less than 1 % over 40 successive iterations; the iterative method saves a factor 10 in computing time for the case quoted in table 1.

We recall a final technical point before proceeding to the description of the results. Triad interactions between modes, k, p, q, can be 'local' (i.e. characteristic scales k^{-1}, p^{-1}, q^{-1} of the same order of magnitude) or 'non-local' (i.e. widely separated scales). The exponential discretization in wavenumbers does not allow for the latter-type interactions (Lesieur & Schertzer 1978). As in I, such non-local interactions have been calculated separately.

3. The critical region

Introduction

Our aim is twofold: determination of the critical magnetic Reynolds number R_c^M above which a magnetic steady state obtains, and study of the supercritical regime ($R^M \gtrsim R_c^M$). The former problem needs only a kinematical framework (the reaction of the magnetic field on the velocity field plays no role), but the latter one must be studied with the full nonlinear equations. However, even in the kinematical case, the linearized EDQNM equations have a complex integrodifferential structure which does not seem to yield analytical results straightforwardly. For that reason, we resorted to a numerical study of the critical region both in the kinematical and in the nonlinear framework. Still two approaches are available to determine R_c^M: temporal evolution towards a steady state or iterative computation. We chose the latter, as it is generally faster. We first give an overview of the parameters which can influence the value of R_c^M in the EDQNM calculations for the non-helical case. The characterization of the supercritical regime ($R^M > R_c^M$) follows; we then proceed to describe the temporal evolution of the system to its steady state and finally reserve a separate paragraph for the helical case.

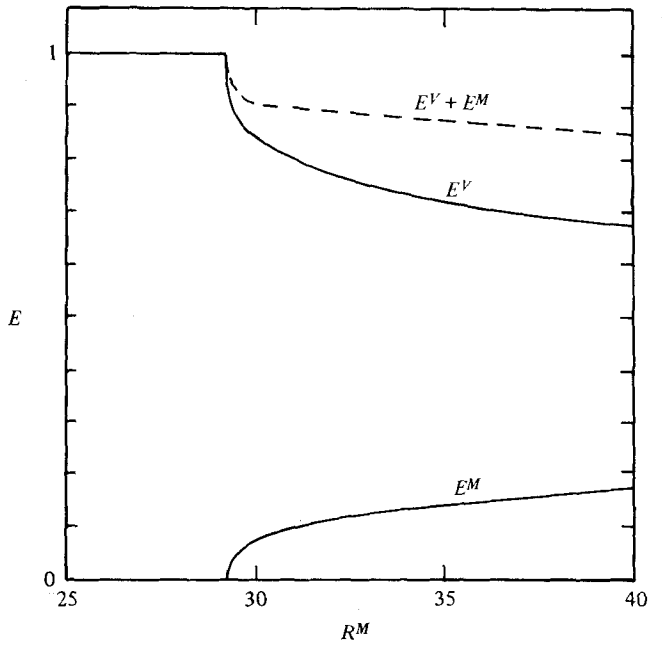

FIGURE 1. Steady-state kinetic (E^V), magnetic (E^M), and total ($E^V + E^M$) energies per unit mass in the critical region (non-helical turbulence; $k_{min}/k_0 = 0{\cdot}25$, $k_{max}/k_0 = 860$; $R^V = 2{\cdot}3 \times 10^4$ in the subcritical state). Notice the bifurcation to a magnetic state that occurs at $R_c^M \simeq 29$.

The critical magnetic Reynolds number

Various quantities relevant to the problem of magnetic criticality are now defined. The kinetic-energy injection spectrum F_k^V is a strongly peaked function around wavenumber k_0 (k_0 is taken equal to unity in the computations). The total kinetic energy injection rate ϵ is given by

$$\epsilon = \int_{k_{\min}}^{k_{\max}} F_k^V \, dk, \tag{3.1}$$

where $k_{\min}$ and $k_{\max}$ are respectively the minimum and maximum wavenumbers. The kinetic Reynolds number R^V, defined in (1.4), is

$$R^V = \left[2 \int_{k_{\min}}^{k_{\max}} E_k^V \, dk\right]^{\frac{1}{2}} \Big/ (k_0 \nu). \tag{3.2}$$

In non-magnetic turbulence, the characteristic rates of nonlinear stretching and of viscous dissipation become roughly equal at the kinetic Kolmogorov dissipation wavenumber

$$k_d^V = (\epsilon/\nu^3)^{\frac{1}{4}}. \tag{3.3}$$

To ensure proper dissipation we need $k_d^V < k_{\max}$. This inequality limits the attainable Reynolds numbers for a given $k_{\max}$. The magnetic Reynolds number R^M is

$$R^M = R^V \nu/\lambda. \tag{3.4}$$

Note that both Reynolds numbers are based on turbulent quantities, r.m.s. velocity and wavenumber of energy-containing eddies. In contrast, the magnetic Reynolds number R_L^M introduced in § 1 is based on mean quantities (mean velocity and overall size of the flow).

R^V	44	$2{\cdot}1 \times 10^3$	10^6
R_c^M	25	29	29

TABLE 2. Variation of the critical magnetic Reynolds number with the kinetic Reynolds number (non-helical turbulence; $k_{\min}/k_0 = 0{\cdot}25$).

$k_{\min}/k_0$	8×10^{-2}	0·25	1	1†
R_c^M	27	29	80	30

† This case has magnetically accessible scales four times larger than kinetic ones (see text).

TABLE 3. Variation of the critical magnetic Reynolds number with the aspect ratio $k_{\min}/k_0$ (non-helical turbulence; $R^V = 2 \times 10^4$). Notice the inhibition of the dynamo effect when the integral scale and the overall size of the flow are comparable ($k_{\min}/k_0 = 1$).

The iterative method described in § 2 is used to obtain the value of the critical magnetic Reynolds number: below R_c^M, the steady state is purely non-magnetic, whereas above R_c^M non-zero magnetic energy obtains in the steady state. Figure 1 shows the stationary kinetic, magnetic and total energies as a function of R^M for a typical case ($k_{\min}/k_0 = 0{\cdot}25$, $R^V \simeq 2{\cdot}3 \times 10^4$). Direct inspection of figure 1 gives a critical magnetic Reynolds number $R_c^M \simeq 29$.

Most determinations to date of the critical magnetic Reynolds number were done in the kinematical framework with a given velocity field made up of a few cells only. The R_c^M found above, on the other hand, is obtained for a fully turbulent flow. As expected the kinetic Reynolds number has very little influence on the critical value of the magnetic Reynolds number (see table 2 for a typical case: $k_{\min}/k_0 = 0{\cdot}25$, $\epsilon = 1$, no helicity). We observe almost no variation of R_c^M in the wide range of kinetic Reynolds numbers explored. This is not surprising since magnetic-energy generation in the critical regime occurs mainly in the energy range ($k \approx k_0$), where the kinetic-energy spectrum is not affected by molecular viscosity. Our result is not consistent with a conjecture of Batchelor (1950) that the critical magnetic Reynolds number should be of the order of the kinetic Reynolds number. Notice that the lowest values of the kinetic Reynolds numbers quoted in table 2 are in the range now accessible by direct numerical simulations of the primitive MHD equations (see § 4).

The precise value of R_c^M may also depend on the energy range through (at least) two parameters: (i) the ratio of the minimum wavenumber $k_{\min}$ to the wavenumber k_0 of energy-containing eddies; (ii) the shape of the energy spectrum. The ratio $k_{\min}/k_0$ is essentially l_0/L, where l_0 is the integral scale of the kinetic turbulence and L the overall size of the system. Table 3 shows the variation of R_c^M with this ratio. A possible interpretation, suggested to us by F. Busse (private communication), is that it is difficult to excite a magnetic field when the flow has essentially only one big eddy ($l_0 \approx L$). Notice however that (in the non-helical case) it hardly matters whether there are 4 or 12 large eddies. The last column of table 3 refers to a case where the overall size of the flow is equal to the injection scale ($l_0 = L$) but the overall size of the conducting (magnetic) region is larger (by a factor 4 in this calculation). This is to some extent the analogue of spherical dynamos with conducting boundaries (Bullard & Gubbins 1977). Currents flowing outside the (kinetic) energy container have a greater scale

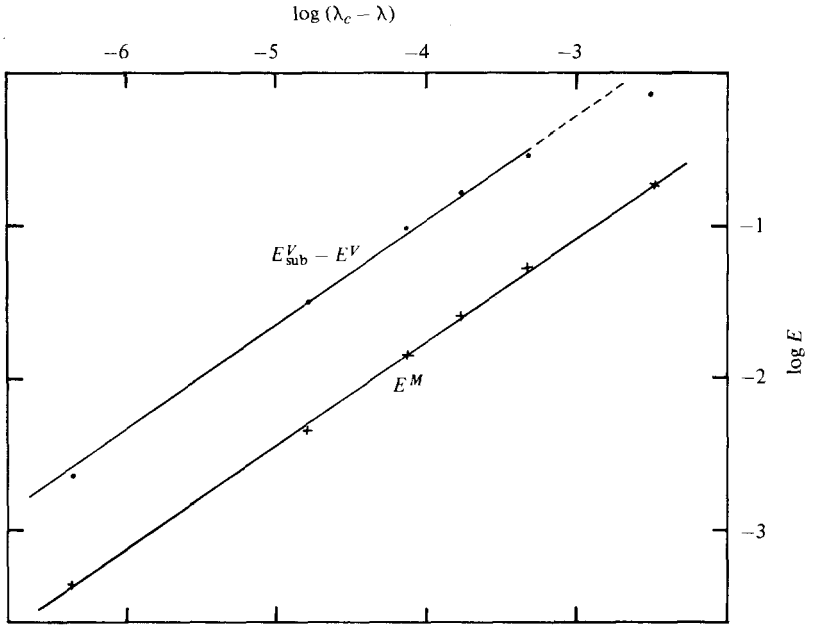

FIGURE 2. Steady-state magnetic energy (E^M) and kinetic-energy deviation from its subcritical value ($E^V_{sub} - E^V$) in the vicinity of the critical magnetic Reynolds number as a function of $\lambda_c - \lambda$ (logarithmic co-ordinates). The straight lines represent power laws $E \sim (\lambda_c - \lambda)^\beta$ with $\lambda_c \simeq (8 \pm 0{\cdot}1) \times 10^{-2}$ and $\beta \simeq 0{\cdot}68 \pm 0{\cdot}05$ (same conditions as in figure 1; $R_c^M \simeq 29{\cdot}2$). This representation is accurate when $(\lambda_c - \lambda)/\lambda_c \lesssim 0{\cdot}1$.

and their characteristic diffusion time is increased, thereby favouring magnetic-energy generation. For example, in a flow with two radial cells, Bullard & Gubbins found that R_{Lc}^M decreases from 57 to 38 when the boundaries turn from isolating to conducting. Although our result (R_c^M decreases from 80 to 30) is obtained under turbulent conditions, we note that the magnitude of the effect is analogous.

We have tested the influence on R_c^M of the shape of the spectral distribution of the kinetic energy by comparing two kinematically prescribed turbulent flows: one with a Kolmogorov range and the other with a flat spectrum extending over two octaves. In both computations the total kinetic energies are the same and $k_{\min}/k_0 = 0{\cdot}25$. In the first case $R_c^M \simeq 29$, whereas in the second $R_c^M \simeq 33$.

Another factor which can affect the critical value of the magnetic Reynolds number through its influence on the kinetic-energy spectrum is the Kolmogorov constant K_0 (which is obtained from experimental data). In the EDQNM calculations, K_0 is related to the adjustable parameter of the closure, the constant C_s appearing in the triad relaxation time (equation (A 19)). In this paper, $C_s = 0{\cdot}26$ corresponding to the commonly accepted value $K_0 = 1{\cdot}4$ (Monin & Yaglom 1975). Other values of the Kolmogorov constant can be simulated by simply adjusting C_s, which in turn modifies R_c^M. For example $K_0 = 1{\cdot}1$, which seems to be an experimental lower bound, yields a critical magnetic Reynolds number $R_c^M \simeq 24$. More details will be given below in the study of the critical region.

To conclude we stress that the critical magnetic Reynolds number for *non-helical* turbulence in the framework of the EDQNM closure is of the order of 30 over a wide

λ	1/12	1/12·6	1/12·7	1/13	1/13·5	1/14	1/15	1/20
E^V	2·76	2·69	2·65	2·54	2·40	2·30	2·17	1·89
E^M	0	0·029	0·045	0·095	0·158	0·204	0·278	0·479
R^M	28·40	29·22	29·25	29·30	29·60	30	31·30	39

TABLE 4. Kinetic and magnetic energies in the critical region (non-helical turbulence, $k_{\min}/k_0 = 0{\cdot}25$). The only external parameter that is varied in these calculations is the magnetic diffusivity λ.

range of parameters. In particular, its dependence on the kinetic Reynolds number is so small that calculations with laminar flows may have some relevance. Note however that the precise way the energy is injected will have some influence. It was already pointed out in § 1 that R_c^M is plausibly larger than 1 because stretching and turbulent magnetic diffusion have comparable characteristic times. The fact that R_c^M is more than one order of magnitude above unity indeed indicates that this competition is a tight one.

The supercritical steady state

We now turn to a more detailed description of the steady state obtained in MHD turbulence with the EDQNM closure. At low magnetic Reynolds numbers, the stationary solution is non-magnetic: for any starting magnetic spectrum, the final state has zero magnetic energy and the kinetic-energy spectrum follows the Kolmogorov law. When R^M grows, a bifurcation occurs in the solution of the spectral equations: the non-magnetic solution turns unstable at $R^M = R_c^M$ and a stable magnetic-energy spectrum is obtained for $R^M > R_c^M$. Table 4 gives the steady-state values of the kinetic and magnetic energies as a function of the magnetic diffusivity λ and the magnetic Reynolds number.

Bifurcation phenomena have generally well-defined exponents. Because of the very unusual structure of the EDQNM equations we have not yet been able to analyse theoretically the neighbourhood of R_c^M. We do however have good numerical evidence that there are simple exponents associated with the R_c^M bifurcation. First, we determine the variation of the steady-state magnetic energy E^M as a function of R^M. For a choice of parameters such that $k_{\min}/k_0 = 0{\cdot}25$, $R^V = 2 \times 10^4$ and $R_c^M = 29$, we obtain, for $R^M > R_c^M$, the empirical law

$$E^M \propto (R^M - R_c^M)^{\beta'}. \tag{3.5}$$

The exponent β' given in table 5 appears to be very sensitive to the value of the Kolmogorov constant K_0. Notice however that R^M is based on the integral scale which itself changes above R_c^M, because the kinetic-energy spectrum changes. A much more nearly universal behaviour obtains in terms of the magnetic diffusivity:

$$E^M \propto (\lambda_c - \lambda)^{\beta}. \tag{3.6}$$

β, given in table 5, is equal to $0{\cdot}68 \pm 0{\cdot}05$ independently of K_0. It appears likely that it is in fact exactly $\frac{2}{3}$. The same exponent holds also for the deviation of the kinetic energy from its subcritical value (see figure 2).

The supercritical steady state is drastically different from the subcritical one, even close to R_c^M. It can be seen on figure 1 that at $R^M = 35$, in a case where $R_c^M = 29$, the magnetic energy represents 17 % of the total energy and the kinetic energy has dropped by 28 % from its subcritical value. This in turn will affect the turbulent transport

K_0	λ_c	β	R_c^M	β'
1·1	0·08	0·68	24	0·32
1·4	0·087	0·68	29	0·50

TABLE 5. Influence of the Kolmogorov constant K_0 on the critical parameters λ_c, β, R_c^M and β'. Note that the critical exponent β seems to be insensitive to K_0.

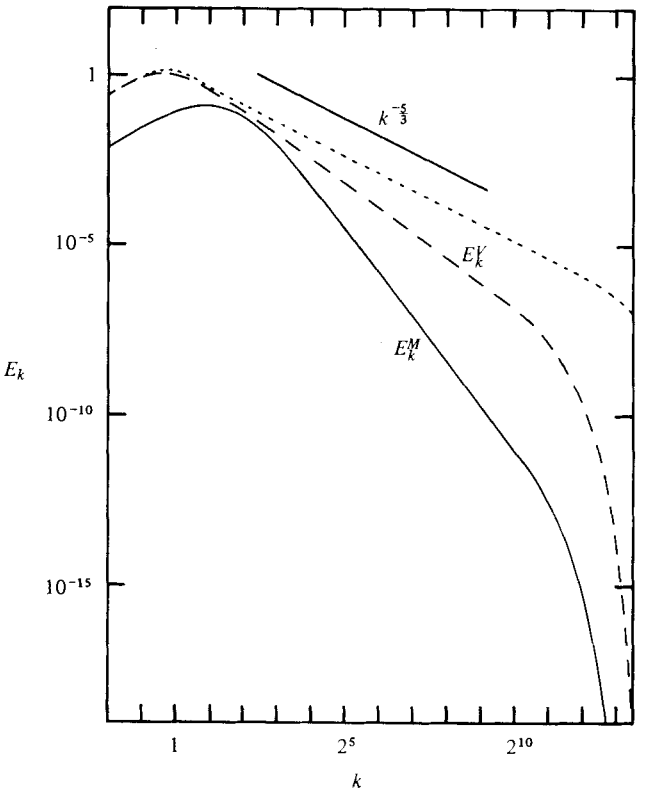

FIGURE 3. Steady-state spectra of magnetic (E_k^M, solid line) and kinetic (E_k^V, dashed line) energies for $R^M \simeq 39$ (non-helical turbulence; $k_{\min}/k_0 = 0{\cdot}25$); the subcritical kinetic-energy spectrum is also shown (dotted line, $E_k^V \sim k^{-m}$, $m \simeq \frac{5}{3}$ in the inertial range). At $R \simeq 39$ ($R_c^M \simeq 29$), there is an inertial range for the kinetic (magnetic) spectrum with exponent $m \simeq 2{\cdot}4$ ($m' \simeq 4{\cdot}4$).

coefficients (such as diffusivity and thermal conductivity) since they depend on the r.m.s. velocity. This point will be discussed further in § 4 as to its consequences for realistic flows in the critical region.

Our closure method allows us to investigate not only overall quantities such as E^V and E^M, but also their detailed spectral distribution. Below R_c^M the kinetic-energy spectrum follows the Kolmogorov law $E_k^V \sim k^{-\frac{5}{3}}$ in the inertial range

$$k_0 \ll k \ll k_d \approx (\epsilon/\nu^3)^{\frac{1}{4}}$$

(see figure 3). Above R_c^M the Lorentz force becomes relevant and we do not *a priori* expect to find a Kolmogorov spectrum. Actually, calculating at $R^M = 39$ in a situation

where $R_c^M \simeq 29$, we found that the kinetic-energy spectrum follows a much steeper power law $E_k^V \sim k^{-m}$ with $m \simeq 2{\cdot}4$; the magnetic-energy spectrum follows an even steeper law $E_k^M \sim k^{-m'}$ with $m' \simeq 4{\cdot}4$ (see figure 3).

We now indicate a possible interpretation of these results. At wavenumbers $k \gg k_0$ the local magnetic Reynolds number is small. Thus the distortion of large-scale magnetic fields by small-scale velocity gradients is strongly limited by Joule dissipation. The resulting small-scale magnetic fields are proportional to the small-scale velocity gradients, the coefficient of proportionality being roughly $b_0/(\lambda k^2)$, where b_0 is the r.m.s. large-scale field. From this we find that

$$E_k^M \approx (b_0/(\lambda k^2))^2 k^2 E_k^V \propto k^{-2} E_k^V. \tag{3.7}$$

This explains that the kinetic- and magnetic-energy spectral exponents differ by exactly two units. The same kind of argument was applied by Golitsyn (1960) and Moffatt (1961) to derive a $k^{-\frac{11}{3}}$ law for E_k^M in the subcritical regime with an external magnetic field. Next, we notice that the dominant contribution to the small-scale Lorentz force comes from the cross-product of large-scale magnetic fields with small-scale currents. Hence the local Lorentz force is proportional to the local velocity amplitude, the coefficient being b_0^2/λ with no k dependence. Actually this is a standard calculation for flows at low magnetic Reynolds number in the presence of a magnetic field (see for example appendix A of Alemany *et al.* 1979). One then finds that the Lorentz force reduces to a linear dissipation term with no k dependence but an angular dependence. For the case of isotropic turbulence, the angular dependence drops out. It seems that competition between nonlinear transfer and such a k-independent dissipation does not lead to the exponential fall-off which obtains for k^2-type diffusive dissipation. More likely, as suggested by Alemany *et al.* (1979), an equilibrium will be achieved between local transfer ($\sim k^{\frac{5}{2}}(E_k^V)^{\frac{3}{2}}$) and dissipation ($\sim E_k^V$); this results in a k^{-3} energy spectrum† (with possible logarithmic corrections). In this context it is of interest to recall that a k^{-3} spectrum has been observed by Alemany *et al.* (1979) in turbulence at low magnetic Reynolds number when the external magnetic field is sufficiently strong. The above argument is only tentative; we notice too that the EDQNM exponent is $m \simeq 2{\cdot}4$, not $m \simeq 3$. It is conceivable that the proximity to R_c^M produces some contamination by the $k^{-\frac{5}{3}}$ subcritical spectrum. This question requires further investigation.

Temporal evolution

To study the approach in time to the steady state, we also perform time-dependent calculations in the critical region. We take as initial conditions a seed magnetic field lying in the energy range ($k \approx k_0$) of a developed hydrodynamical turbulence with a Kolmogorov spectrum. The total magnetic energy is $E^M = 10^{-3}E^V$ at $t = 0$ and we vary the magnetic diffusivity λ. Figure 4 shows the time evolution of the total magnetic energy for various λ; even when $R^M < R_c^M$, there is at first a growth of the magnetic energy. This lasts only a few large eddy-turnover times. A similar increase is also found in two-dimensional turbulence at high kinetic and magnetic Reynolds numbers (Pouquet 1978), although it is known that the steady state is non-magnetic. For $R^M < R_c^M$, all the magnetic modes will eventually decay and the magnetic energy drops to zero. For $R^M > R_c^M$, the magnetic steady state that occurs is found to be

† Notice also that the k^{-3} spectrum will be cut off by viscosity at wavenumbers such that the viscous diffusion time $(\nu k^2)^{-1}$ becomes smaller than the turnover time $(k^3 E_k^V)^{-\frac{1}{2}}$.

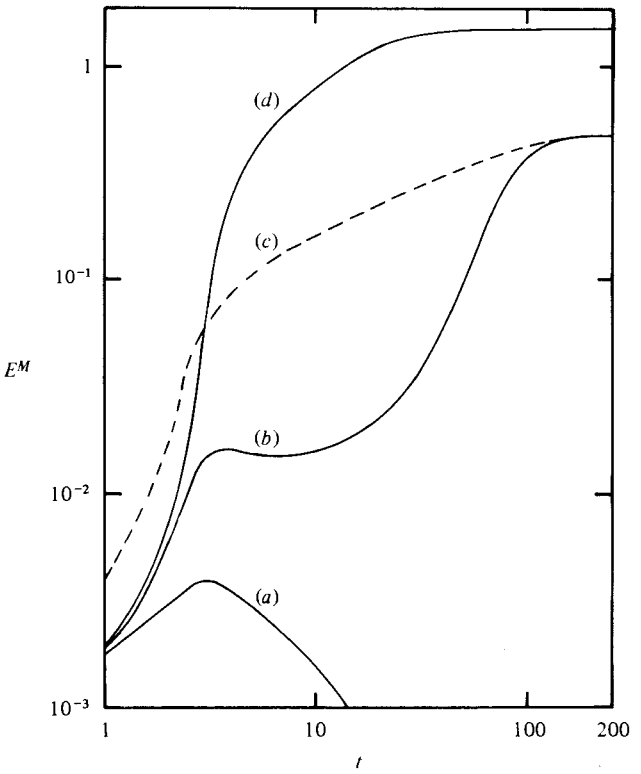

FIGURE 4. Evolution of the magnetic energy for different magnetic diffusivities. The time is in units of the eddy-turnover time at wavenumber k_0 (ratio of magnetic to kinetic energy initially 10^{-3}). (*a*) $\lambda = 0{\cdot}1$, the magnetic energy eventually decreases to zero. (*b*), (*c*) $\lambda = 0{\cdot}05$, the steady state is magnetic. For (*b*) $E_k^M(t=0) \propto k^4 \exp(-2k^2)$ and for (*c*) the initial magnetic energy is concentrated at $k = k_0 = 1$. (*d*) $\lambda = 3 \times 10^{-3}$ (case studied in I). Notice the common short growth until $t \simeq 3$ and the long time required to reach saturation above R_c^M.

independent of the initial magnetic-energy spectrum (compare in figure 4 curve *b* for which $E_k^M(t=0) \propto k^4 \exp(-2k^2)$ and curve *c* for which the initial magnetic energy is concentrated in a single mode $k = k_0$). Notice that, close to R_c^M, the time scale to reach the steady state becomes very long. This 'critical slowdown', due to the fact that an eigenvalue of the linearized equation crosses the value zero, makes the time-integration method much slower than the iterative method for the determination of the critical magnetic Reynolds number. Figure 5 gives the kinetic and magnetic energy spectra for different times when the magnetic Reynolds number is 43 ($R_c^M \simeq 29$). The initial kinetic-energy spectrum is of the Kolmogorov type, $(E^M/E^V)_{t=0} = 10^{-3}$, with the initial magnetic energy concentrated in the large scales ($k \approx k_0$). At first, the magnetic energy spreads towards the small scales, until it reaches the dissipation scale. In the next phase the magnetic energy experiences a slower exponential growth: in the example of figure 5, the total magnetic energy is amplified by an order of magnitude between $t = 10$ and $t = 60$. At $t = 60$ the ratio E^M/E^V is 5×10^{-2}; the characteristic growth time is only weakly dependent on wavenumber in the energy range and is roughly 21 turnover times. At later times the Lorentz force becomes significant; the kinetic-energy spectrum steepens (see preceding paragraph) and the growth rate of the magnetic energy drops to zero.

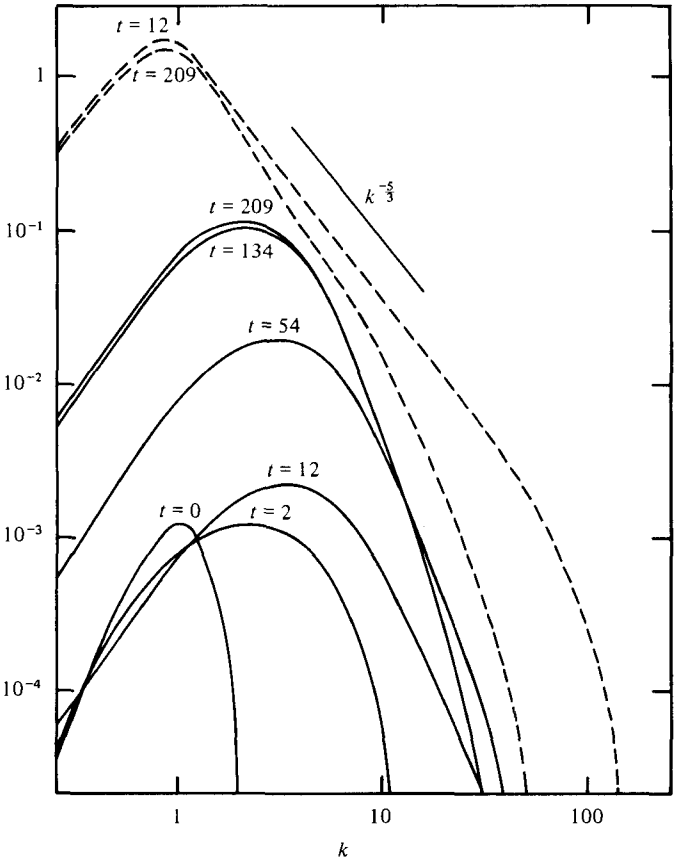

FIGURE 5. Kinetic- (dashed lines) and magnetic- (solid lines) energy spectra (non-helical turbulence; $k_{\min}/k_0 = 0{\cdot}25$) for different times. Initial conditions: developed kinetic spectrum ($R^V \simeq 2{\cdot}1 \times 10^3$) and $(E^M/E^V)_{t=0} = 10^{-3}$ ($E^M_k(t=0) \propto k^4 \exp(-2k^2)$). Notice the decrease of the kinetic energy in the small scales.

λ	10^{-1}	5×10^{-2}	3×10^{-2}	3×10^{-3}	10^{-6}
$(\epsilon/\lambda^3)^{\frac{1}{4}}/k_0$	5·6	9·5	14	78	$3{\cdot}2 \times 10^4$
k_0^M/k_0	2	3·4	4·8	6	8

TABLE 6. Influence of magnetic diffusivity on the wavenumber k_0^M of maximum magnetic-energy growth.

As a last point, let us mention, as it may be interesting for experimental purposes, the dependence of the wavenumber k_0^M of maximum magnetic-energy growth upon the magnetic diffusivity λ. This is shown in table 6 above. Note that this result does not seem to be consistent with the scaling $k_0^M \sim (\epsilon/\lambda^3)^{\frac{1}{4}}$ proposed by Kraichnan & Nagarajan (1967).

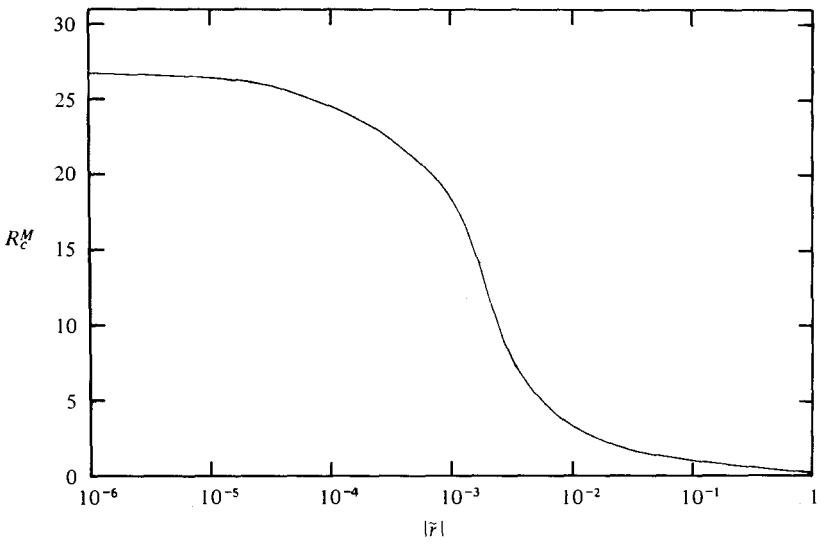

FIGURE 6. Variation of the critical magnetic Reynolds number with the relative rate of helicity injection $\tilde{r}$ ($0 \leqslant |\tilde{r}| \leqslant 1$) when scale separation holds ($k_{\min}/k_0 = 8 \times 10^{-3}$). Critical magnetic Reynolds numbers below unity are obtained when $|\tilde{r}| \gtrsim 0{\cdot}1$.

Influence of helicity

When the overall size of the system is much greater than a typical kinetic-energy-containing scale ($k_{\min} \ll k_0$), it is known (see § 1) that kinetic helicity plays an important role in the generation of large-scale magnetic fields. In the linear theory, after averaging over small scales of helical turbulence, an $\alpha \nabla \times \mathbf{b}$ term which destabilizes the large scales appears in the induction equation (Steenbeck *et al.* 1966). We therefore expect that the critical magnetic Reynolds number is reduced when the turbulence is helical. In the nonlinear regime helical turbulence will not produce indefinite growth of the magnetic field: as shown in I saturation comes about from an interplay of kinetic helicity, magnetic helicity and Alfvén waves.

We investigate the dependence of R_c^M on helicity by using the helical EDQNM spectral equations (see appendix); in non-mirror symmetric turbulence, the forcing correlation function includes a pseudo-scalar contribution corresponding to the helicity injection spectrum $\tilde{F}_k^V$. The total rate of helicity injection $\tilde{\epsilon}$ is defined as

$$\tilde{\epsilon} = \int_{k_{\min}}^{k_{\max}} \tilde{F}_k^V \, dk. \tag{3.8}$$

We choose the relative rate of helicity injection $\tilde{r}$ ($0 \leqslant |\tilde{r}| \leqslant 1$)

$$\tilde{r} = \tilde{F}_k^V / (k F_k^V) \tag{3.9}$$

to be independent of wavenumber. When $|\tilde{r}| = 1$, helicity is said to be injected at maximal rate.

We first consider the variation of R_c^M with the relative rate of helicity injection $\tilde{r}$ when there is a wide scale separation ($k_{\min}/k_0 = 8 \times 10^{-3}$). Figure 6 shows a rather sharp changeover of roughly one order of magnitude in R_c^M around $\tilde{r} \simeq 10^{-3}$; we stress that even a very small amount of helicity leads to strong reduction in R_c^M; for

$k_{\min}/k_0$	8×10^{-3}	0·25	1
$\tilde{r}=0$	27	29	80
$\tilde{r}=1$	0·3	2	13

TABLE 7. Influence of helicity on the critical magnetic Reynolds number for various ratios $k_{\min}/k_0$. $\tilde{r}=0$, no helicity; $\tilde{r}=1$, maximal helicity.

example, for $\tilde{r}=10^{-2}$, $R_c^M\simeq 3$ ($R_c^M\simeq 27$ in the non-helical case). Notice also that the critical magnetic Reynolds number has dropped below unity in the case of maximal helicity injection ($\tilde{r}=1$). As already seen from the phenomenological analysis of § 1, we expect to find arbitrarily low values of R_c^M as $k_{\min}/k_0\to 0$: for sufficiently small wavenumbers, the growth rate of the helicity instability, having a linear k dependence, will overcome the turbulent diffusivity rate.

What happens now if there is little or no scale separation? Surprisingly we found that helicity is still a significant parameter in its ability to reduce R_c^M (compare $\tilde{r}=0$ and $\tilde{r}=1$ in table 7). The fact that the critical magnetic Reynolds number is strongly reduced in helical turbulence, even when scale separation does not hold, should simplify further experimental and/or numerical investigations of the critical regime. This will be examined further in the following section.

4. Summary, discussion and conclusion

In this paper we have addressed the problem of magnetic criticality in turbulent conducting flows. We now first summarize the results obtained in § 3 using the eddy-damped quasi-normal Markovian (EDQNM) closure and then proceed to more general discussions and conclusions.

The closure calculation assumes homogeneous isotropic three-dimensional MHD turbulence with periodic boundary conditions (the period L is thus the largest available scale). Energy and (possibly) helicity are injected by prescribed random forces stirring the fluid at scales $\approx l_0$ (integral scale). The essential parameters of the problem are l_0/L, the kinetic and magnetic Reynolds numbers $R^V=l_0v_0/\nu$ and $R^M=l_0v_0/\lambda$ and the relative rate of helicity injection $\tilde{r}$, defined by (3.9). The basic question is: when will an initially weak magnetic perturbation be amplified and lead to a steady state with non-vanishing magnetic energy?

The main results are listed below:

(1) In all cases, including non-helical turbulence, a stationary magnetic state exists when R^M exceeds a critical value R_c^M. In the non-helical case, R_c^M is typically of the order of a few tens.

(2) R_c^M is asymptotically independent of R^V when the latter is large enough. For example, $R_c^M\simeq 25$ for $R^V=44$ and $R_c^M\simeq 29$ for $R^V=10^6$ ($l_0/L=0{\cdot}25$; no helicity).

(3) In the non-helical case R_c^M is asymptotically independent of L as $l_0/L\to 0$. For example, $R^M\simeq 80$ for $l_0=L$, $R_c^M\simeq 29$ for $l_0/L=0{\cdot}25$ and $R_c^M\simeq 27$ for $l_0/L\ll 1$.

(4) In the helical case ($0<|\tilde{r}|\leqslant 1$), R_c^M can become very small when the largest-scale L in the system greatly exceeds the integral scale l_0. There is good evidence that $R_c^M\to 0$ as $l_0/L\to 0$ as suggested by the phenomenological analysis of § 1. For example when $\tilde{r}=1$ (maximal helicity injection) and $l_0/L=8\times10^{-3}$ we obtain $R_c^M\simeq 0{\cdot}3$.

More surprising, we found that, when l_0 and L are comparable, helicity still strongly affects the value of R_c^M; for example with $l_0 = L$, the critical magnetic Reynolds number drops by a factor of 6 when the relative helicity injection rate varies from 0 to 1.

(5) Above R_c^M a non-zero magnetic energy E^M (per unit mass) obtains, the kinetic energy E^V drops and so does the total energy $E^T = E^V + E^M$ (see figure 1). For example, at $R^M = 35$ in a situation where $R_c^M \simeq 29$, $\tilde{r} = 0$, $l_0/L = 0{\cdot}25$, the kinetic energy is down by 28 % from its subcritical value and the total energy is down by 13 %. A substantial decrease of the turbulent transport coefficients of heat, momentum, etc. is therefore expected.

(6) Near R_c^M, the behaviour of E^M can be empirically represented by a power law, $E^M \propto (\lambda_c - \lambda)^\beta$ ($\beta \simeq 0{\cdot}68 \pm 0{\cdot}05$, possibly equal to 2/3).

(7) The kinetic-energy spectrum E_k^V which follows a Kolmogorov $k^{-\frac{5}{3}}$ law below R_c^M changes over, immediately above R_c^M, to a much steeper power law with an exponent $m \simeq 2{\cdot}4$. The magnetic-energy spectrum E_k^M has an exponent $m' \simeq m + 2$ (see figure 3).

Concerning all the above results, we must stress that their qualitative aspects (e.g. the more or less pronounced effect of varying the parameters) seem much more reliable than their quantitative aspects (e.g. the precise value of R_c^M for a given set of parameters), since they are not derived from the primitive MHD equations. It is clear that our study, based on a closure, leaves room for improvement. A first step would be to resort to direct numerical simulation of the MHD equations without leaving the framework of homogeneous isotropic, randomly driven turbulence with periodic boundary conditions. In the non-turbulent kinematical case such calculations have already been made and produced critical magnetic Reynolds numbers of the order of 10 for two velocity modes (Roberts 1972). In the turbulent case, assuming that result 2 above carries over to the primitive equations, calculations at kinetic Reynolds numbers of the order of 40 should give (within less than 20 %) the critical magnetic Reynolds number corresponding to the limit $R^V \to \infty$. Kinetic Reynolds numbers of the order of 40 are precisely within the range accessible to existing high-speed computers. We recall that Pouquet & Patterson (1978) have made a simulation of the MHD equations with R^V and R^M up to 30 (32^3 grid points). They did not investigate criticality (no random force to drive the flow), but some of their results indicate that a seed magnetic field can be substantially amplified at such Reynolds numbers. On the CDC 7600 which they used, a typical run took about one hour and required a considerable amount of data management. On a fast vectorized computer such as CRAY 1, a 32^3 MHD calculation can be made entirely in core and requires less than one minute per turnover time; for a dynamo run several tens of turnover times are needed. Furthermore, a 64^3 calculation becomes now accessible (again with extensive data management and run times of the order of ten hours or more). At this resolution the Reynolds number can probably be pushed from 30 (corresponding to 32^3) to $30 \times 2^{\frac{4}{3}}$ or $30 \times 2^{\frac{5}{3}}$ before truncation effects are felt.†

Such magnetic Reynolds numbers are in all probability supercritical in the non-helical case (if criticality obtains at all in homogeneous turbulence) and are most

† The former value (76) is based on the Kolmogorov (1941) assumption that the dissipation wavenumber scales like the $\frac{3}{4}$th power of the Reynolds number; the latter value (85) is based on Kraichnan's (1965) modification for MHD.

certainly supercritical in the helical case. Simulations can also be used to investigate other interesting phenomena outside the scope of the EDQNM closure: is there a symmetry breaking mechanism leading to a preferred direction of the supercritical magnetic field (as in the ferromagnetic phase transition)? Is the transition sharp (as in the closure calculation or in condensed-matter critical phenomena) or will the magnetic field appear in the form of intermittent bursts with R_c^M possibly equal to zero when the forcing is Gaussian?

We come now to the more speculative question of the possible inferences of our results for 'realistic' flows with boundaries, inhomogeneities, mean flow, etc. For non-magnetic turbulence at high Reynolds numbers, there is good evidence that the small-scale motion away from boundaries is adequately described as homogeneous isotropic turbulence. In the supercritical MHD case, homogeneity will also probably hold at small scales but isotropy need not (because a large-scale magnetic field, unlike a large-scale velocity field, cannot be gauged out by a Galilean transformation). At such scales, where the local magnetic Reynolds number is small, existing experimental results on low magnetic Reynolds number turbulence with an external magnetic field (Alemany *et al.* 1979) may become relevant (see § 3). What about the large scales which are, near R_c^M, mostly responsible for magnetic field generation? We feel confident that most of the closure-based qualitative results will carry over to realistic flows. In particular we expect (and conjecture) that R_c^M can be substantially decreased by making the flow helical, including in the case when there is no clear-cut separation between the integral scale of the turbulence and the overall scale of the flow. Concerning actual values of R_c^M for realistic flows we cannot make any predictions. We just wish to point out that critical magnetic Reynolds numbers in the same range (10 to 10^2) as in the present study are obtained in kinematic dynamo calculations with prescribed non-turbulent velocity fields and non-periodic (generally spherical) geometry (Gubbins 1973; Pekeris *et al.* 1973).

A particularly important class of 'realistic' flows, which indirectly motivated the present study, are found in large-scale liquid-sodium cooling circuits of breeder reactors (Vendryes 1977). For Superphenix, under construction at Malville (France), the magnetic Reynolds number R_L^M, in the secondary pumps, based on $L = 2{\cdot}5$ m, maximum velocity $V = 5$ m s^{-1}, and magnetic diffusivity $\lambda = 0{\cdot}16$ m^2 s^{-1} (operating temperature 345 °C) will be $R_L^M = 79$. We do not see how to rule out criticality under such conditions. It is noteworthy that the primary circuit flow is helical at small scales in the core because spacing of fuel pins is ensured by helical wires; there may also be some large-scale helicity induced by either the pumps or the coils of the heat exchangers. Furthermore, as noticed by R. Moreau (1979, private communication), the magnetic Reynolds number based on the overall size of the primary liquid-sodium circuit is of the order of 100 and there may be co-operative effects between different portions of the circuit.

Let us tentatively examine some of the possible consequences of supercriticality (in the magnetic, not the nuclear sense). Steady or fluctuating magnetic fields of the order of 100 gauss may be present as soon as R_c^M is exceeded by more than a few per cent (this is based on the observation that, with a mean velocity of 1 m s^{-1}, equipartition of kinetic and magnetic energy at 400 °C occurs for 330 gauss). Such fields may lead to problems with the control system (in electromagnetic flowmeters for example), pressure drops, additional oscillations and vibrations (especially if the magnetic field comes in

bursts) and possibly extra corrosion induced by electric currents. Some of these problems have already been mentioned by Bevir (1973). Furthermore the drop in kinetic energy, which will most certainly accompany magnetic-energy generation, may result in decreased efficiency of heat transfer, thereby requiring more energetic pumping to remove the energy released in the core.

There are at least two methods that can be helpful in finding out whether or not a given reactor will be in the supercritical regime: numerical simulation and extrapolation of subcritical experiments on relaxation of magnetic perturbations.

Numerical simulations to find R_c^M can be done in the kinematic dynamo framework. Determination of the full subcritical velocity field, to feed into such a calculation, appears neither feasible nor necessary. The mean flow which possesses rather strong gradients in places (pumps, bends, entrance and exit points from main vessel) may be sufficient to trigger self-excitation. The main difficulties will come from the need to accommodate complicated boundary conditions (portions or the entirety of the primary circuit can be simulated) and to have sufficient resolution to push R^M to critical values without truncation effects.

In attempting to experimentally determine the critical value of the magnetic Reynolds number, the following observation may be of use: in the subcritical regime $R^M < R_c^M$ (but not too far from R_c^M), the rate of relaxation of an externally imposed magnetic perturbation depends linearly† on the magnetic diffusivity λ and vanishes at the critical value. R_c^M can then be determined by extrapolation. This method has been suggested by W. Malkus (private communication). He used it in trying to determine R_c^M for a flow in a rotating and precessing sphere (unpublished results corresponding to the liquid-sodium version of the experiment reported in Malkus 1968). This procedure might be usefully attempted with the scaled-down version of Superphenix, the Phenix breeder which operates at Marcoule (France) with magnetic Reynolds numbers about half of those of the Superphenix breeder. As noticed by Bevir (1973), decreasing the sodium temperature from 400 °C to, say, 150 °C will decrease the magnetic diffusivity by roughly a factor 2. The magnetic Reynolds number of Phenix can thus be brought to a value closer to the Superphenix operating conditions. Alternatively, one can set up liquid-sodium experiments specifically designed to study magnetic criticality (Gailitis & Freiberg 1977). The results suggest that the scaling up from Phenix to Superphenix may produce adverse consequences; it does not seem possible, in the present state of knowledge, to prove that this will not happen.

We are indebted to F. Busse, R. Kraichnan, O. Lielausis, R. Moreau, P.-L. Sulem and W. Malkus for useful discussions. We wish particularly to thank D. Gillet who performed most of the helical calculations. The helpful observations of the referees are acknowledged.

† This simply expresses the fact that there is a crossing of zero by the real part of an eigenvalue of the induction operator in equation (1.2). Since this operator is linear in λ, the range over which this eigenvalue is approximately linear may be greater in the variable λ than in its inverse, R^M.

Appendix

The EDQNM spectral equations for helical MHD turbulence were derived in Pouquet *et al.* (1976); they can be written in the following form:

$$(\partial/\partial t + 2\nu k^2)\, E_k^V = \mathscr{B}_k^V + \mathscr{A}_k^V E_k^V + \tilde{\mathscr{A}}_k^V H_k^V + F_k^V, \tag{A 1}$$

$$(\partial/\partial t + 2\nu k^2)\, H_k^V = \tilde{\mathscr{B}}_k^V + k^2 \tilde{\mathscr{A}}_k^V E_k^V + \mathscr{A}_k^V H_k^V + \tilde{F}_k^V, \tag{A 2}$$

$$(\partial/\partial t + 2\lambda k^2)\, E_k^M = \mathscr{B}_k^M + \mathscr{A}_k^M E_k^M + k^2 \tilde{\mathscr{A}}_k^M H_k^M, \tag{A 3}$$

$$(\partial/\partial t + 2\lambda k^2)\, H_k^M = \tilde{\mathscr{B}}_k^M + \tilde{\mathscr{A}}_k^M E_k^M + \mathscr{A}_k^M H_k^M, \tag{A 4}$$

where a tilde denotes a pseudo-scalar quantity.

The emission and absorption terms are given by

$$\mathscr{B}_k^V = k^3 \int_{\Delta_k} \frac{dp\,dq}{pq} [\theta_{kpq}^V (b_{kpq} E_p^V E_q^V - c_{kpq} p^{-2} H_p^V H_q^V) + \theta_{kpq}^{VM} c_{kpq} (E_p^M E_q^M - q^2 H_p^M H_q^M)], \tag{A 5}$$

$$\tilde{\mathscr{B}}_k^V = k^3 \int_{\Delta_k} \frac{dp\,dq}{pq} [\theta_{kpq}^V (b_{kpq} H_p^V E_q^V - c_{kpq} E_p^V H_q^V) + \theta_{kpq}^{VM} f_{kpq} kp H_p^M E_q^M], \tag{A 6}$$

$$\mathscr{B}_k^M = k^3 \int_{\Delta_k} \frac{dp\,dq}{pq} \theta_{kpq}^{VM} [c_{kpq} k^2 p^{-2} E_p^V E_q^M + h_{kpq} (E_p^M E_q^V + q^2 p^{-2} H_p^V H_q^M)], \tag{A 7}$$

$$\tilde{\mathscr{B}}_k^M = k^3 \int_{\Delta_k} \frac{dp\,dq}{pq} \theta_{kpq}^{VM} h_{kpq} (H_p^M E_q^V + p^{-2} H_p^V E_q^M), \tag{A 8}$$

$$\mathscr{A}_k^V = -k \int_{\Delta_k} \frac{dp\,dq}{pq} [\theta_{kpq}^V b_{kpq} p^2 E_q^V + \theta_{kpq}^{VM} c_{kpq} p^2 E_q^M], \tag{A 9}$$

$$\tilde{\mathscr{A}}_k^V = k \int_{\Delta_k} \frac{dp\,dq}{pq} \theta_{kpq}^V c_{kpq} H_q^V, \tag{A 10}$$

$$\mathscr{A}_k^M = -k \int_{\Delta_k} \frac{dp\,dq}{pq} \theta_{kpq}^{VM} (h_{kpq} p^2 E_q^V + c_{kpq} k^2 E_q^M), \tag{A 11}$$

$$\tilde{\mathscr{A}}_k^M = k^{-1} \int_{\Delta_k} \frac{dp\,dq}{pq} \theta_{kpq}^{VM} (e_{kpq} p^3 q H_q^M - h_{kpq} p^2 H_q^V), \tag{A 12}$$

The different terms used in these expressions are defined below: E_k^V and E_k^M are the kinetic- and magnetic-energy spectra, the total energy per unit mass being

$$\tfrac{1}{2}(\langle v^2 \rangle + \langle b^2 \rangle) = \int_0^\infty dk\, (E_k^V + E_k^M); \tag{A 13}$$

H_k^V is the kinetic helicity spectrum with

$$\tfrac{1}{2}\langle \mathbf{v} \,.\, \mathrm{curl}\, \mathbf{v} \rangle = \int_0^\infty H_k^V\, dk; \tag{A 14}$$

and H_k^M is the magnetic helicity spectrum with

$$\tfrac{1}{2}\langle \mathbf{a} \,.\, \mathbf{b} \rangle = \int_0^\infty dk\, H_k^M; \tag{A 15}$$

where $\mathbf{a}$ is the vector potential ($\mathbf{b} = \mathrm{curl}\, \mathbf{a}$).

The kinetic energy and helicity are injected at rates ϵ and $\tilde{\epsilon}$,

$$\epsilon = \int_0^\infty dk\, F_k^V, \quad \tilde{\epsilon} = \int_0^\infty dk\, \tilde{F}_k^V; \tag{A 16}$$

F_k^V and $\tilde{F}_k^V$ are peaked at $k = k_0$, decreasing rapidly at high wavenumbers,

$$F_k^V \sim k^4 \exp(-2(k/k_0)^2).$$

In the computations, ϵ and k_0 are taken equal to unity.

Δ_k is a subset of the (p, q) plane such that k, p and q can form a triangle. The geometric coefficients appearing in the equations above are

$$b_{kpq} = pk^{-1}(xy + z^3), \quad c_{kpq} = pk^{-1}z(1-y^2),$$
$$e_{kpq} = x(1-z^2), \quad f_{kpq} = z - xy - 2zy^2, \quad h_{kpq} = 1-y^2, \tag{A 17}$$

where x, y, z are the cosines of the angles opposite to the sides k, p, q of the triangle.

The EDQNM equations of second-order moments contain either purely kinetic or mixed (kinetic, magnetic) triple correlations for which we obtain two types of linear relaxation: the kinetic transfer terms involve only molecular viscosity, whereas all other transfers involve both molecular viscosity and magnetic diffusivity. In order to ensure realizability of the energy spectra we choose (see I) the kinetic and mixed triad relaxation rates μ_{kpq}^V and μ_{kpq}^{VM} to be symmetric in wavenumber, namely

$$\mu_{kpq}^X = \mu_k^X + \mu_p^X + \mu_q^X, \tag{A 18}$$

where X stands for either V or VM, with

$$\mu_k^V = \nu k^2 + C_s\left[\int_0^k dq\, q^2(E_q^V + E_q^M)\right]^{\frac{1}{2}} + 3^{-\frac{1}{2}}k\left[\int_0^k dq E_q^M\right]^{\frac{1}{2}}, \tag{A 19}$$

$$\mu_k^{VM} = \mu_k^V + \lambda k^2; \tag{A 20}$$

$C_s = 0{\cdot}26$ gives a Kolmogorov constant of 1·4 in the absence of magnetic field.

The triad relaxation times used in the EDQNM equations are then defined as usual by

$$\theta_{kpq}^X = [1 - \exp(-(t\mu_{kpq}^X))]/\mu_{kpq}^X, \tag{A 21}$$

with $X = V$ or VM. When $\lambda \gg \nu$, i.e. for small magnetic Prandtl numbers, it is important to make a distinction between the two triad relaxation times θ^V and θ^{VM}.

The stationary equations for the kinetic and magnetic energy and helicity spectra are given below in the form used in the iterative scheme:

$$E_k^V = [(\mathscr{B}_k^V + F_k^V)(-\mathscr{A}_k^V + 2\nu k^2) + (\tilde{\mathscr{B}}_k^V + \tilde{F}_k^V)\tilde{\mathscr{A}}_k^V]/\mathscr{D}_k^V, \tag{A 22}$$

$$H_k^V = [(\mathscr{B}_k^V + F_k^V)k^2\tilde{\mathscr{A}}_k^V - (\tilde{\mathscr{B}}_k^V + \tilde{F}_k^V)(\mathscr{A}_k^V - 2\nu k^2)]/\mathscr{D}_k^V, \tag{A 23}$$

$$E_k^M = [\mathscr{B}_k^M(-\mathscr{A}_k^M + 2\lambda k^2) + k^2\tilde{\mathscr{B}}_k^M\tilde{\mathscr{A}}_k^M]/\mathscr{D}_k^M, \tag{A 24}$$

$$H_k^M = [\mathscr{B}_k^M\tilde{\mathscr{A}}_k^M - \tilde{\mathscr{B}}_k^M(\mathscr{A}_k^M - 2\lambda k^2)]/\mathscr{D}_k^M, \tag{A 25}$$

where

$$\mathscr{D}_k^V = (\mathscr{A}_k^V - 2\nu k^2)^2 - k^2(\tilde{\mathscr{A}}_k^V)^2, \tag{A 26}$$

$$\mathscr{D}_k^M = (\mathscr{A}_k^M - 2\lambda k^2)^2 - k^2(\tilde{\mathscr{A}}_k^M)^2. \tag{A 27}$$

The EDQNM equations are used in this paper both in their helical form given above, and in their mirror-symmetric form (with all the H^V and H^M terms set equal to zero). The non-helical equations can also be found in Kraichnan & Nagarajan (1967). Note several differences between the equations in table 1 of I and in this appendix. The magnetic forcing terms F_k^M and $\tilde{F}_k^M$ are here identically zero. There were misprints in three transfer terms of I which are corrected below. (We are grateful to Dr De Young

for pointing out to us those misprints.) They involved the expressions of T^V_{VM}, $T^V_{\tilde{V}\tilde{V}}$, $T^{\tilde{V}}_{V\tilde{V}}$ which should read:

$$T^V_{VM} = -kpq^{-1}c_{kpq}E^M_q E^V_k;$$

$$T^V_{\tilde{V}\tilde{V}} = -kq^{-1}p^{-3}c_{kpq}(k^2H^V_p H^V_q - p^2H^V_q H^V_k);$$

$$T^{\tilde{V}}_{V\tilde{V}} = kp^{-1}q^{-1}b_{kpq}(k^2H^V_p E^V_q - p^2E^V_q H^V_k) - k^3p^{-1}q^{-1}c_{kpq}(E^V_p H^V_q - H^V_q H^V_k).$$

Moreover, the constant C_s (related to the Kolmogorov constant) should read: $C_s = 0{\cdot}26$ (and not $C_s = 0{\cdot}36$). Finally, as indicated above, for a small magnetic Prandtl number, one has to take into account the magnetic diffusive damping time, thus introducing a modification in the triple correlation relaxation time θ_{kpq}.

REFERENCES

Alemany, A., Moreau, R., Sulem, P.-L. & Frisch, U. 1979 *J. Méc.* **18**, 277.

Backus, C. E. 1958 *Ann. Phys.* **4**, 372.

Batchelor, G. K. 1950 *Proc. Roy. Soc.* A **201**, 405.

Bevir, M. K. 1973 *J. British Nucl. Energy Soc.* **12**, 455.

Biermann, L. & Schlüter, A. 1951 *Phys. Rev.* **82**, 863.

Bullard, E. C. & Gubbins, D. 1977 *Geophys. Astrophys. Fluid Dyn.* **8**, 43.

Busse, F. H. 1978 *Ann. Rev. Fluid Mech.* **10**, 435.

Childress, S. 1969 Théorie magnétohydrodynamique de l'effet dynamo. *Dép. Méc. Fac. Sci., Paris.*

Frisch, U., Sulem, P.-L. & Nelkin, M. 1978 *J. Fluid Mech.* **87**, 719.

Gailitis, A. & Freiberg, Ya. 1977 Calculation of helical flux dynamo instability. *Rep. Phys. Inst., Latvian Acad. Sci. Riga, U.S.S.R.*

Gailitis, A., Freiberg, Ya. & Lielausis, O. A. 1977 On the observations of the magnetic field generation in liquid sodium flows. *Rep. Phys. Inst., Latvian Acad. Sci. Riga, U.S.S.R.*

Golitsyn, G. S. 1960 *Dokl. Akad. Nauk S.S.S.R.* **132**, 315. (English transl. 1960 *Sov. Phys. Dokl.* **5**, 536.)

Gubbins, D. 1973 *Phil. Trans. Roy. Soc.* A **274**, 493.

Kolmogorov, A. N. 1941 *Dokl. Akad. Nauk S.S.S.R.* **32**, 19.

Kolmogorov, A. N. 1962 *J. Fluid Mech.* **13**, 82.

Kraichnan, R. H. 1958 *Phys. Rev.* **109**, 1407.

Kraichnan, R. H. 1965 *Phys. Fluids* **8**, 1385.

Kraichnan, R. H. & Nagarajan, S. 1967 *Phys. Fluids* **10**, 859.

Launder, B. E., Reece, G. J. & Rodi, W. 1975 *J. Fluid Mech.* **68**, 537.

Leith, C. E. 1971 *J. Atmos. Sci.* **28**, 145.

Léorat, J., Pouquet, A. & Frisch, U. 1980 *J. Phys.* **41** (C3), 359,

Lesieur, M. & Schertzer, D. 1978 *J. Méc.* **17**, 609.

Leslie, D. C. 1973 *Developments in the Theory of Turbulence.* Clarendon.

Lorenz, E. N. 1963 *J. Atmos. Sci.* **20**, 130.

Malkus, W. V. R. 1968 *Science* **160**, 259.

Martin, P. C. 1976 *J. Phys. Coll.* **37**, C1.

Moffatt, H. K. 1961 *J. Fluid Mech.* **11**, 625.

Moffatt, H. K. 1978 *Magnetic Field Generation in Electrically Conducting Fluids.* Cambridge University Press.

Monin, A. & Yaglom, A. M. 1975 *Statistical Fluid Mechanics: Mechanics of Turbulence*, vol. II (ed. J. L. Lumley). Massachusetts Institute of Technology Press.

Orszag, S. A. 1970 *J. Fluid Mech.* **41**, 363.

ORSZAG, S. A. 1977 Statistical theory of turbulence in fluid dynamics. In *Les Houches Summer School of Theoretical Physics* (eds. R. Balian & J. L. Peube). Gordon and Breach.

ORSZAG, S. A. & KRUSKAL, M. D. 1968 *Phys. Fluids* **11**, 43.

PEKERIS, C. L., ACCAD, Y. & SHKOLLER, B. 1973 *Phil. Trans. Roy. Soc.* A **275**, 425.

PIERSON, E. S. 1975 *Nucl. Sci. & Engng* **57**, 155.

POUQUET, A. 1978 *J. Fluid Mech.* **88**, 1.

POUQUET, A. 1980 Fully developed magnetohydrodynamic turbulence. Numerical simulation and closure techniques. Preprint Observatoire de Nice.

POUQUET, A., FRISCH, U. & LÉORAT, J. 1976 *J. Fluid Mech.* **77**, 321.

POUQUET, A. & PATTERSON, G. S. 1978 *J. Fluid Mech.* **85**, 305.

ROBERTS, G. O. 1972 *Phil. Trans. Roy. Soc.* A **271**, 411.

ROSE, H. A. & SULEM, P.-L. 1978 *J. Phys.* **39**, 461.

RUELLE, D. & TAKENS, F. 1971 *Commun. Math. Phys.* **20**, 167; erratum **23**, 343.

STEENBECK, M., KRAUSE, F. & RÄDLER, K. H. 1966 *Z. Naturforsch.* A **21**, 369. (English transl. in Roberts, P. H. & Stix, M. 1971 *National Center for Atmos. Res. Tech. Note no.* 11–60, Boulder, Colorado, U.S.A.)

VENDRYES, G. A. 1977 *Sci. American* **236** (3), 8.

VON NEUMANN, J. 1949 Recent theories of turbulence. *Collected Works* **6**, 437.

ZEL'DOVICH, YA. B. 1956 *Zh. Exp. Teor. Fiz.* **31**, 154. (English transl. 1957 *Sov. Phys. J. Exp. Theor. Phys.* **4**, 460.)

Note added in proof (11 December 1980)

Direct numerical simulations of the kind suggested in §4 have been performed recently. Gilman & Miller (preprint, High Altitude Observatory, Boulder, Colorado, 1980) have obtained a nonlinear dynamo driven by thermal convection in a rotating spherical shell. Frisch, Meneguzzi & Pouquet (unpublished, 1980), using resolutions of 32^3 and 64^3 have obtained both helical and non-helical homogeneous dynamos at magnetic Reynolds numbers up to 100; the results are in good agreement with the closure predictions of the present paper and of paper I, and additional features, such as intermittency, are detected.